# Spatiotemporal Coherent Control of Light through a Multiple Scattering Medium with the Multispectral Transmission Matrix

Mickael Mounaix,[1,*] Daria Andreoli,[1,2] Hugo Defienne,[1] Giorgio Volpe,[1,3]
Ori Katz,[1,2,4] Samuel Grésillon,[2] and Sylvain Gigan[1]

[1]*Laboratoire Kastler Brossel, ENS-PSL Research University, CNRS, UPMC Sorbonne Universités, Collège de France, 24 rue Lhomond, 75005 Paris, France*

[2]*Sorbonne Universités, UPMC Univ Paris 06, UMR 7587, Institut Langevin, 1 rue Jussieu, F-75005, Paris, France*

[3]*Department of Chemistry, University College London, 20 Gordon Street, London WC1H 0AJ, United Kingdom*

[4]*Department of Applied Physics, The Selim and Rachel Benin School of Computer Science and Engineering, The Hebrew University of Jerusalem, Jerusalem 9190401, Israel*

(Received 22 December 2015; revised manuscript received 4 March 2016; published 21 June 2016)

We report the broadband characterization of the propagation of light through a multiple scattering medium by means of its multispectral transmission matrix. Using a single spatial light modulator, our approach enables the full control of both the spatial and spectral properties of an ultrashort pulse transmitted through the medium. We demonstrate spatiotemporal focusing of the pulse at any arbitrary position and time with any desired spectral shape. Our approach opens new perspectives for fundamental studies of light-matter interaction in disordered media, and has potential applications in sensing, coherent control, and imaging.

DOI: 10.1103/PhysRevLett.116.253901

Propagation of coherent light through a scattering medium produces a speckle pattern at the output [1], due to light scrambling by multiple scattering events [2]. The phase and amplitude information of the light are spatially mixed, thus limiting the resolution, depth, and contrast of most optical imaging techniques. Ultrashort pulses, generated by broadband mode-locked lasers, are very useful for multiphotonic imaging and nonlinear physics [3–5]. In the temporal domain, an ultrashort pulse is temporally broadened during propagation in a scattering medium, due to the long dwell time within it [6,7], which therefore limits its range of applications.

However, this scattering process is linear and deterministic. Therefore, one can control the input wave front to design the output field. In this respect, spatial light modulators (SLMs) offer more than a million degrees of freedom to control the propagation of coherent light. These systems have played an important role in the development of wave front shaping techniques to manipulate light in complex media. Iterative optimization algorithm [8–10] and phase conjugation methods [11,12] have been proposed to focus light at a given output position, an essential ingredient for imaging. An alternative method for light control is the optical transmission matrix (TM). The TM is a linear operator that links the input field (SLM) to the output field (CCD camera) [13,14]. The measurement of the TM allows imaging through [15] or inside a scattering medium [16], and potentially access to the mesoscopic properties of the system [17].

The possibility of shaping the pulse in time is also essential for coherent control [18]. Temporally, photons exit a scattering medium at different times, giving rise to a broadened pulse at its output [7,19]. The temporal spreading of the original pulse is characterized by a confinement time $\tau_m$ [20] related to the Thouless time [21]. Equivalently, from a spectral point of view, the scattering medium responds differently for the distinct spectral components of an ultrashort pulse, with a spectral correlation bandwidth $\Delta\omega_m \propto 1/\tau_m$, giving rise to a very complex spatiotemporal speckle pattern [22–25]. With a single SLM, one can manipulate the spatial degrees of freedom to adjust the delay between different optical paths. Therefore, the spatial and temporal distortions can both be compensated using wave front shaping techniques. This approach allows the temporal compression of an ultrashort pulse at a given position by iteratively optimizing the input wave front [26–28], or alternatively by using digital phase conjugation [29]. Another technique consists in shaping only the spectral profile of the pulse at the input, to compensate the temporal distortion induced by the medium [30]. Equivalently to a spectral approach, the measurement of a time-resolved reflection matrix [31,32] enables light delivery at a given depth of the scattering medium.

Recently, the measurement of a TM of the medium for several wavelengths, the multispectral transmission matrix (MSTM) [22], allowed for both spatial and spectral control at any position in space using a single SLM. In Ref. [22], since the spectral phase relation between different matrices was unknown, deterministic temporal control was still elusive. Here, we introduce the MSTM formalism including the spectral phase relation between the different frequency responses of the medium. This additional information gives access to a full spatiotemporal control of an ultrashort pulse propagating in the disordered medium.

 

We demonstrate the deterministic spatiotemporal focusing and enhanced excitation of a nonlinear process. Beyond this dispersion compensation process, we also deterministically shape the temporal profile of the output pulse.

First, we need to describe the propagation of an ultrashort pulse through the scattering medium, i.e., measure the MSTM. The ratio between the spectral bandwidth of the ultrashort pulse $\Delta\omega_L$ and $\Delta\omega_m$ gives the number of independent spectral degrees of freedom $N_\omega$. It corresponds to the number of monochromatic TMs that one needs to measure to completely describe both spatially and spectrally the propagation of the broadband signal. In Ref. [22], the reference signal in the measurement of the MSTM was a copropagative speckle, as in Ref. [14]. Since this reference speckle is also $\lambda$ dependent, the spectral phase remained undetermined. Nonetheless, the manipulation of the input field with this incomplete MSTM allows using the scattering medium as a very complex optical component, such as a lens or a grating [22]. Achieving full control of the pulse in the time domain requires the knowledge of the relative phase relation between the wavelengths of the pulse at the output of the medium. Here, the reference field is a plane wave of known phase introduced by an external reference arm. This reference field is common to all the individual monochromatic TMs: the relative phase between the different wavelengths of the output pulse is then accessible in every spatial position at the output. The output field reads

$$E_j^{\text{out}} = \sum_{i=1}^{N_{\text{SLM}}} \sum_{k=1}^{N_\omega} h_{jik} e^{i\varphi_{jk}} E_i^{\text{in}}(\lambda_k), \tag{1}$$

where $E_j^{\text{out}}$ represents the value of the output field at the $j$th pixel of the CCD camera, $E_i^{\text{in}}(\lambda_k)$ represents the value of the input field at the $i$th SLM pixel at wavelength $\lambda_k$, and $h_{jik}e^{i\varphi_{jk}}$ represent the coefficients of the MSTM with $\varphi_{jk}$ the spectral phase component.

Figure 1 illustrates the experimental setup. A Ti:sapphire laser source (MaiTai, Spectra Physics) produces a 110 fs ultrashort pulse, centered at 800 nm with a spectral bandwidth of 10 nm FWHM. The same laser can also be used as a tunable monochromatic laser in the same spectral range. The phase-only SLM (LCOS-SLM, Hamamatsu X10468) is used in reflection, subdivided in $32 \times 32$ macropixels, which is a good compromise between the duration of the measurement of the MSTM and the efficiency of the focusing process. The scattering medium is a thick layer of ZnO nanoparticles randomly distributed on a glass slide, placed between two microscope objectives. Most experiments are performed on an approximately

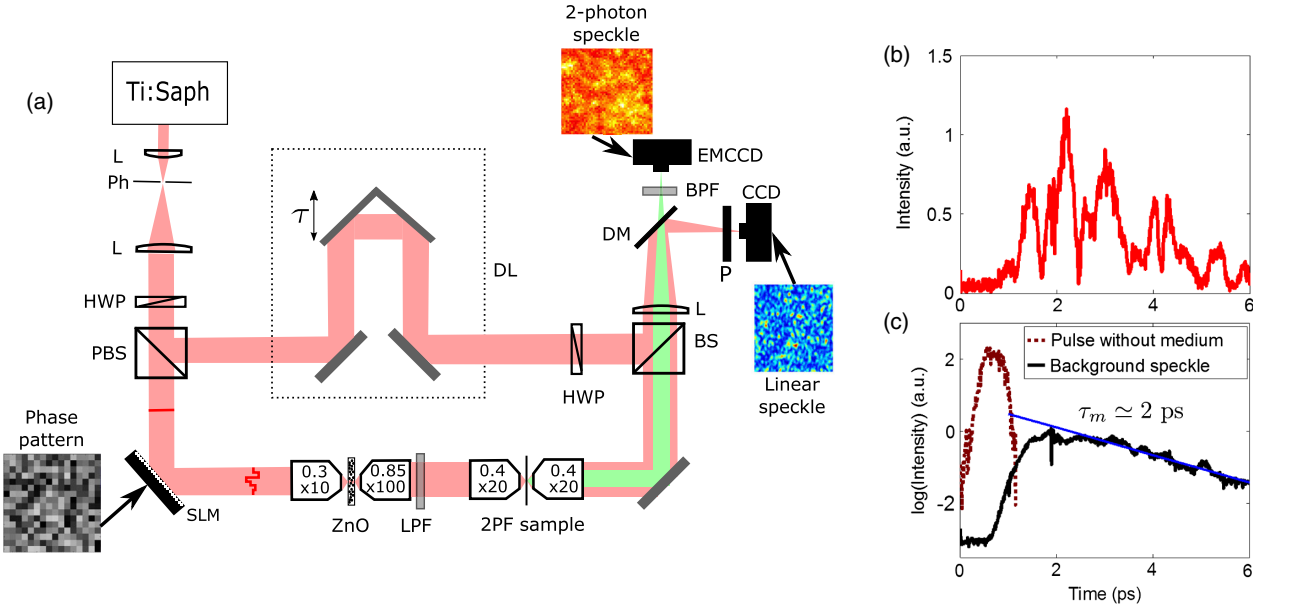


FIG. 1. Principle of the experiment. (a) Experimental setup. The laser (ultrashort pulse 110 fs at FWHM) is expanded and illuminates the SLM, which is conjugated with the back focal plane of a microscope objective. The scattering medium is a thick (around 100 $\mu$m) sample of ZnO nanoparticles, placed between two microscope objectives. The output plane is imaged on the two-photon fluorescence (2PF) sample. The long-pass filter (LPF) allows one to eliminate the autofluorescence of the ZnO. A dichroic mirror (DM) separates the two-photon fluorescence signal [imaged with an electron multiplying charge coupled device (EMCCD) camera] from the linear signal (imaged with a CCD). Lens ($L$), pinhole (Ph), half plate wave (HPW), polarized beam splitter (PBS), delay line (DL), beam splitter (BS), polarizer ($P$), band pass filter (BPF). (b) Temporal speckle from a single spatial speckle grain, obtained with an Interferometric Cross-Correlation (ICC) measurement. (c) ICC of the original pulse in the sample arm without the medium (dotted line), characterized by a time width of 520 fs at FWHM. ICC of the transmitted pulse through the medium, averaged over 100 different spatial positions of the speckle (solid line), characterized by a decay time of $\simeq$2 ps (blue line).

100 $\mu$m thick sample, characterized by its spectral correlation bandwidth $\Delta\lambda_m \simeq 0.5$ nm (measurement done in the same way as Ref. [22]), equivalent to $\Delta\omega_m \simeq 3$ THz. The two paths have the same optical length: when the laser is generating an ultrashort pulse, both the ultrashort reference pulse and the stretched one are overlapped in space and time. The output plane of the scattering medium is imaged on a two-photon fluorescent sample, which is a powder of fluorescein diluted in ethanol, inside a glass capillary (CM Scientific, 20 $\mu$m $\times$ 200 $\mu$m $\times$ 5 cm). The excitation of this nonlinear process will be used to differentiate the spatiotemporal from the spatial focusing. A longpass filter is placed between the two sets of microscope objectives to eliminate some residual autofluorescence of the scattering medium. A CCD camera records the linear output intensity, and is used to measure the MSTM. The two-photon signal is recorded with an EMCCD camera, placed after a dichroic mirror to separate the linear signal from the fluorescence. In a first step, the laser is set to cw, and we measured the MSTM for $N_\omega = 21$ wavelengths in a 13-nm spectral window centered at 800 nm. In essence, for each wavelength, we display a series of phase patterns on the SLM, and for each input pattern, phase stepping holography with the external reference arm wave permits us to recover the complex output field. The MSTM is deduced from this set of measurement. Once the MSTM has been measured, the laser is set back to pulsed operation. The CCD camera integrates the output speckle over time and only recovers its spatial fluctuations. The temporal shape of the speckle is retrieved with an interferometric cross-correlation (ICC) measurement between the stretched pulse and an ultrashort reference by scanning the reference arm. The temporal envelope of this signal is then retrieved by applying a low pass filter in the Fourier domain [33].

The temporal envelope of an output signal recorded at one given spatial position (one speckle grain) is shown on Fig. 1(b). The measured output pulse is strongly elongated compared to the initial signal and it shows a very complex temporal structure. Averaging over 100 different output positions allows us to recover a smooth shape [Fig. 1(c)]. Its linear decay rate gives access to the confinement time $\tau_m \simeq 2$ ps corresponding to the time of flight distribution of the photons inside the medium. The value obtained is in agreement with the spectral correlation bandwidth $\Delta\omega_m$ independently measured. This averaged envelope can be compared to the envelope of the pulse reconstructed without the scattering medium. The ultrashort pulse in the reference arm is transform limited at 110 fs, whereas the same pulse after propagation in the sample arm is dispersed to a time width of 520 fs at FWHM (mainly because of the microscope objectives).

At this stage, we want to use the MSTM to generate a particular temporal profile at a given output spatial position. The input pattern to focus a given wavelength $\lambda_k$ at a given position can be simply obtained by phase conjugating the corresponding line of the monochromatic TM ($\lambda_k$) [14], thus generating a focus without any temporal compression. To extend this idea to the temporal domain, we can generalize this principle. It is possible, using a single SLM pattern, to focus multiple wavelengths $\lambda_k$ simultaneously at a given position, with a well-defined spectral phase $\theta_k$. The corresponding solution can be obtained by algebraically summing all the individual patterns. Since the SLM is phase only, the optimal phase pattern to display is simply the argument of the solution. For example, to achieve spatiotemporal focusing, each frequency is focused into a specific output spatial position, while simultaneously ensuring that their relative phases are equal: $\theta_1 = \cdots = \theta_{N_\omega}$.

The main result is presented in Fig. 2, where we demonstrate the temporal compression of the pulse. The presented temporal profiles are retrieved with an ICC measurement. All data are averaged over nine different spatial positions at the output for better visibility. Imposing a flat spectral phase (i.e., the same spectral phase for all wavelengths) at a chosen spatial position at the output, we observe spatiotemporal focusing at a time determined by the delay line position where the MSTM was previously measured, corresponding to the top arrow in Fig. 2. Temporal compression of the output pulse is obtained almost to its Fourier limited time width (120 fs at FHWM). The shape of the pulse around the peak is not due to artifacts but is due to the square spectral window used in the MSTM measurement, giving a cardinal sine form with an expected rebound at 400 fs from the arrival time of the pulse. As a comparison, spatial focusing is also demonstrated by focusing only the central wavelength of the output pulse [34]. The observed intensity is higher than the averaged background speckle because the pulse is spatially focused, but temporal compression is missing.

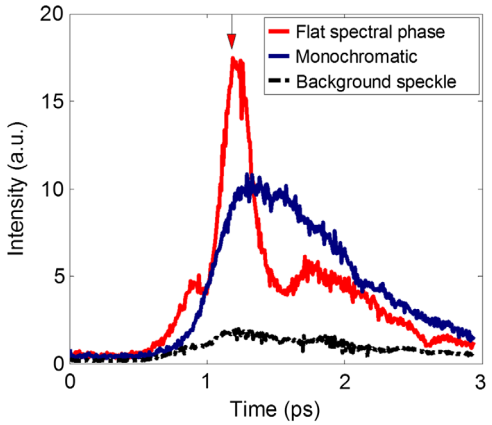


FIG. 2. Spatiotemporal focusing with the MSTM, averaged over nine different spatial positions at the output. Spatiotemporal focusing is achieved by imposing a flat spectral phase at the output, whereas spatial focusing is obtained by focusing only the central wavelength of the pulse. The MSTM was measured at a delay-line position corresponding to the top arrow.

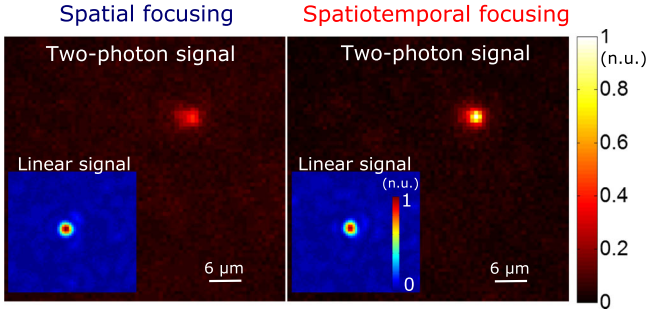


FIG. 3. Comparison of two-photon excitation for spatial (monochromatic phase conjugation) and spatiotemporal focusing, obtained with a thinner scattering sample of ZnO ($\tau_m \simeq 500$ fs). Inset: corresponding CCD signal. Integration time identical for both excitations: 2s for the two-photon excitation and 1 ms for the linear excitation. Scale bars normalized to the maximum intensity of spatiotemporal focusing. We observe a twofold enhancement of the nonlinear signal for the same average intensity when performing spatiotemporal focusing.

To unequivocally demonstrate the temporal compression, we complement our linear ICC characterization by a two-photon fluorescence measurement. The total intensity of the two-photon fluorescent signal is proportional to the square of the excitation intensity, and also to the inverse of its time width [35]. Therefore, with an equivalent spatial focusing, a temporal compression corresponds to a higher two-photon signal. In Fig. 3, we show the two fluorescent signals related to input wave fronts that give either spatial-only (signal-to-background ratio: 8.5) or spatiotemporal focusing (signal-to-background ratio: 19.6) at the output of the medium, with a thinner scattering sample of ZnO (characterized by a measured $\Delta\lambda_m \simeq 2$ nm, requiring the use of six monochromatic TMs) to increase the two-photon signal contrast. The signal over noise ratio of the two-photon signal is about 2.5 times higher when the light is spatiotemporally focused compared to the case where the light is spatially focused, with a similar linear signal and the same focus spot size in both cases [36].

The MSTM gives also access to a more sophisticated spectral shape. The control of this information allows any kind of spectral shape at the output of the scattering medium [37], without any additional measurement. In essence, the scattering medium in conjunction with the spatial light modulator can be used as a pulse shaper. Results of temporal control on the output signal are shown in Fig. 4 [38]. In Figs. 4(a) and 4(b) a linear spectral phase relation $\theta$ between the wavelengths of the pulse is imposed, thus advancing or delaying the arrival time of the pulse. By tuning the slope of the imposed spectral phase ramp [37], the ultrashort pulse can be temporally shifted with a controllable delay

$$\tau = -\frac{\delta\phi\lambda_0^2}{2\pi c\delta\lambda}, \tag{2}$$

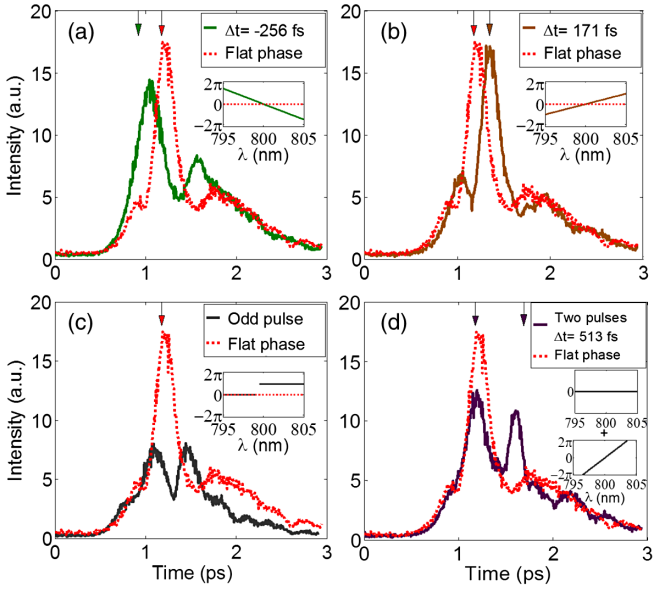


FIG. 4. Any suitable spectral shape can be obtained. (a) A negative spectral phase ramp advances the arrival time of the pulse. (b) A positive spectral phase ramp delays the pulse. (c) A $\pi$-phase step in the spectral domain creates an odd pulse. (d) The sum of a flat phase pulse and a spectral phase ramp pulse gives two pulses with a controlled delay at the same output spatial position. Inset: spectral phase profile applied to the signals. The top arrows indicate the expected arrival time of the pulse.

where $\delta\phi$ is a phase difference between the first and the last wavelength in a spectral interval $\delta\lambda$ centered around $\lambda_0$, and $c$ is the speed of light. The predicted arrival time of the pulse is indicated by the top arrows on each plot. The ultrashort pulse is focused in the same output spatial position, but its arrival time is changed. Two other important examples are demonstrated. First, a $\pi$-phase step between the two halves of the spectrum induces a pulse with a dip, also called an odd pulse [39,40], which can be extremely useful for coherent control [41]. The corresponding temporal profile is presented in Fig. 4(c). Second, a linear superposition of a flat phase pulse and a spectral phase ramp pulse on the SLM at the same spatial position allows the arrival of two pulses with a controllable delay as the two solutions are incoherent with themselves because of the temporal speckle. This could allow pump-probe excitation. As an example, we show in Fig. 4(d) two pulses separated by $\Delta t = 513$ fs.

In all these experiments, the efficiency of the focusing, i.e., the signal to background ratio of the obtained spatiotemporal shape relative to the background speckle, scales linearly with the number of controllable degrees of freedom, here the number of controlled segments on the SLM [26]. It also depends on the number of different spatial targets [8,14] and temporal targets, and on the number of spectral degrees of freedom $N_\omega$ [42].

In conclusion, our setup allows us to access both the spatial and spectral phase information of the MSTM, thus

using the multiple scattering medium in conjunction with the SLM as a lens and a pulse shaper. It is also conceivable to focus two pulses at two different times at two different spatial positions, or to control the duration of the pulse by adding a quadratic phase relation between the frequencies. As these examples indicate, any temporal shape is achievable, with a resolution given by the temporal duration of the pulse, over a temporal interval related to the confinement time of the medium and limited spatially by the speckle grain size. It can be achieved using only the spatial degrees of freedom of a single SLM. This temporal control could enable coherent quantum control [43], or the excitation of localized nano objects, and open interesting perspectives for the study of light-matter interaction and nonlinear imaging in multiple scattering media, and more fundamental insights such as light transport properties [44].

The authors would like to thank Thomas Chaigne for inspiring discussions. This work was funded by the European Research Council (Grant No. 278025). S. G. is a member of the Institut Universitaire de France.

*mickael.mounaix@lkb.ens.fr

[1] J. W. Goodman, J. Opt. Soc. Am. **66**, 1145 (1976).
[2] P. Sebbah, Waves and Imaging through Complex Media (Springer, Netherlands, 2001).
[3] M. Oheim, E. Beaurepaire, E. Chaigneau, J. Mertz, and S. Charpak, J. Neurosci. Methods **111**, 29 (2001).
[4] W. Denk, J. Strickler, and W. Webb, Science **248**, 73 (1990).
[5] T. Brabec, and F. Krausz, Rev. Mod. Phys. **72**, 545 (2000).
[6] N. C. Bruce, F. E. W. Schmidt, J. C. Dainty, N. P. Barry, S. C. W. Hyde, and P. M. W. French, Appl. Opt. **34**, 5823 (1995).
[7] P. M. Johnson, A. Imhof, B. P. J. Bret, J. G. Rivas, and A. Lagendijk, Phys. Rev. E **68**, 016604 (2003).
[8] I. M. Vellekoop, and A. P. Mosk, Opt. Lett. **32**, 2309 (2007).
[9] I. M. Vellekoop, and A. P. Mosk, Phys. Rev. Lett. **101**, 120601 (2008).
[10] I. M. Vellekoop, and A. P. Mosk, Opt. Commun. **281**, 3071 (2008).
[11] I. N. Papadopoulos, S. Farahi, C. Moser, and D. Psaltis, Opt. Express **20**, 10583 (2012).
[12] Z. Yaqoob, D. Psaltis, M. S. Feld, and C. Yang, Nat. Photonics **2**, 110 (2008).
[13] C. W. J. Beenakker, Rev. Mod. Phys. **69**, 731 (1997).
[14] S. M. Popoff, G. Lerosey, R. Carminati, M. Fink, A. C. Boccara, and S. Gigan, Phys. Rev. Lett. **104**, 100601 (2010).
[15] S. Popoff, G. Lerosey, M. Fink, A. C. Boccara, and S. Gigan, Nat. Commun. **1**, 1 (2010).
[16] T. Chaigne, O. Katz, A. C. Boccara, M. Fink, E. Bossy, and S. Gigan, Nat. Photonics **8**, 58 (2014).
[17] A. Goetschy, and A. D. Stone, Phys. Rev. Lett. **111**, 063901 (2013).
[18] J. M. Dela Cruz, I. Pastirk, M. Comstock, V. V. Lozovoy, and M. Dantus, Proc. Natl. Acad. Sci. U.S.A. **101**, 16996 (2004).
[19] M. Tomita, and T. Matsumoto, J. Opt. Soc. Am. B **12**, 170 (1995).
[20] N. Curry, P. Bondareff, M. Leclercq, N. F. van Hulst, R. Sapienza, S. Gigan, and S. Grésillon, Opt. Lett. **36**, 3332 (2011).
[21] D. J. Thouless, Phys. Rep. **13**, 93 (1974).
[22] D. Andreoli, G. Volpe, S. Popoff, O. Katz, S. Grésillon, and S. Gigan, Sci. Rep. **5**, 10347 (2015).
[23] A. P. Mosk, A. Lagendijk, G. Lerosey, and M. Fink, Nat. Photonics **6**, 283 (2012).
[24] E. Small, O. Katz, Y. Guan, and Y. Silberberg, Opt. Lett. **37**, 3429 (2012).
[25] F. van Beijnum, E. G. van Putten, A. Lagendijk, and A. P. Mosk, Opt. Lett. **36**, 373 (2011).
[26] J. Aulbach, B. Gjonaj, P. M. Johnson, A. P. Mosk, and A. Lagendijk, Phys. Rev. Lett. **106**, 103901 (2011).
[27] H. P. Paudel, C. Stockbridge, J. Mertz, and T. Bifano, Opt. Express **21**, 17299 (2013).
[28] O. Katz, E. Small, Y. Bromberg, and Y. Silberberg, Nat. Photonics **5**, 372 (2011).
[29] E. E. Morales-Delgado, S. Farahi, I. N. Papadopoulos, D. Psaltis, and C. Moser, Opt. Express **23**, 9109 (2015).
[30] D. J. McCabe, A. Tajalli, D. R. Austin, P. Bondareff, I. A. Walmsley, S. Gigan, and B. Chatel, Nat. Commun. **2**, 447 (2011).
[31] Y. Choi, T. R. Hillman, W. Choi, N. Lue, R. R. Dasari, P. T. C. So, W. Choi, and Z. Yaqoob, Phys. Rev. Lett. **111**, 243901 (2013).
[32] S. Kang *et al.*, Nat. Photonics **9**, 253 (2015).
[33] A. Monmayrant, S. Weber, and B. Chatel, J. Phys. B **43**, 103001 (2010).
[34] See Supplemental Material at http://link.aps.org/supplemental/10.1103/PhysRevLett.116.253901, Sec. D, part 1, for a comparison between monochromatic and polychromatic focusing in order to achieve spatial-only focusing.
[35] W. R. Zipfel, R. M. Williams, and W. W. Webb, Nat. Biotechnol. **21**, 1369 (2003).
[36] See Supplemental Material at http://link.aps.org/supplemental/10.1103/PhysRevLett.116.253901, part 2, for further explanations on why both spatial and spatio-temporal focusing have the same linear enhancement.
[37] A. M. Weiner, Rev. Sci. Instrum. **71**, 1929 (2000).
[38] See Supplemental Material at http://link.aps.org/supplemental/10.1103/PhysRevLett.116.253901, part 1, for more details on how the MSTM is used to perform the pulse shaping presented in Fig. 4.
[39] A. M. Weiner, and J. P. Heritage, Rev. Phys. Appl. **22**, 1619 (1987).
[40] A. M. Weiner, D. E. Leaird, J. S. Patel, and J. R. Wullert, IEEE J. Quantum Electron. **28**, 908 (1992).
[41] D. Meshulach, and Y. Silberberg, Phys. Rev. A **60**, 1287 (1999).
[42] F. Lemoult, G. Lerosey, J. de Rosny, and M. Fink, Phys. Rev. Lett. **103**, 173902 (2009).
[43] Y. Silberberg, and D. Meshulach, Nature (London) **396**, 239 (1998).
[44] J. Wang, and A. Z. Genack, Nature (London) **471**, 345 (2011).